

# Synthetic Advances Inspired by the Bioactive Dinitrosyl Iron Unit

Published as part of the Accounts of Chemical Research special issue "Synthesis in Biological Inorganic Chemistry".

Randara Pulukkody and Marcetta Y. Darensbourg\*

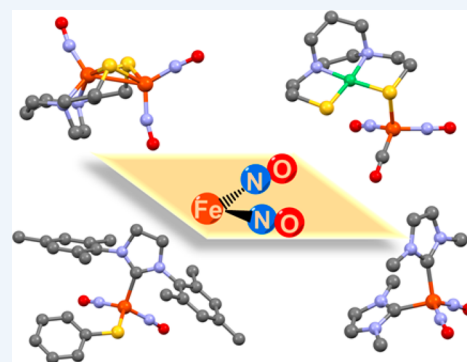
Department of Chemistry, Texas A&M University, College Station, Texas 77843, United States

**CONSPECTUS:** Resulting from biochemical iron–NO interactions, dinitrosyl iron complexes (DNICs) are small organometallic-like molecules, considered to serve as vehicles for NO transport and storage *in vivo*. Formed by the interaction of NO with cellular iron sulfur clusters or with the cellular labile iron pool, DNICs have been documented to be the largest NO-derived adduct in cells, even surpassing the well-known nitrosothiols (RSNOs). Continuing efforts in biological chemistry are aimed at understanding the movement of DNICs in and out of cells, and their important role in NO-induced iron efflux leading to apoptosis in cells.

Intrigued by the integrity of the unique dinitrosyl iron unit (DNIU) and the possibility of roles for it in human physiology or medicinal applications, the understanding of fundamental properties such as ligand effects on its ability to switch between two redox levels has been pursued through biomimetic complexes. Using metallocenes and N-heterocyclic carbenes (NHCs) as ligands to  $\text{Fe}(\text{NO})_2$ , the synthesis of a library of novel DNICs, in both the oxidized,  $\{\text{Fe}(\text{NO})_2\}^9$ , and reduced,  $\{\text{Fe}(\text{NO})_2\}^{10}$ , forms (Enemark–Feltham notation), offers opportunity to examine structural, reactivity, and spectroscopic features.

The *raison d'être* for the  $\text{Mn}_2\text{S}_2\cdot\text{Fe}(\text{NO})_2$  synthesis development is for the potential to exploit the ease of accessing two redox levels on two different metal sites, a property presumably required for achieving two electron redox processes in base metals. Hence such molecules may be viewed as synthetic analogues of [NiFe]- or [FeFe]-hydrogenase active sites in nature, both of which use bridging thiolates for connection of the two centers. A particular success was the development of an  $\text{Fe}(\text{NO})\text{N}_2\text{S}_2\cdot\text{Fe}(\text{NO})_2^{+/0}$  redox pair for proton reduction electrocatalysis.

Monomeric, reduced NHC-DNICs of the  $\text{L}_2\text{Fe}(\text{NO})_2$  type are synthesized via the  $\text{Fe}(\text{CO})_2(\text{NO})_2$  precursor, and oxidized thiolate-containing forms are derived from the dimeric  $(\mu\text{-RS})_2[\text{Fe}(\text{NO})_2]_2$ . Monomeric NHC-DNICs are four coordinate, pseudotetrahedral compounds with planar  $\text{Fe}(\text{NO})_2$  units in which the slightly bent Fe–NO groups are directed symmetrically inward at both redox levels. They serve as stable analogues of biological histidine binding sites. In agreement with IR data, Mössbauer spectroscopic parameters, and DFT computations, the prototypic NHC-DNICs indicate extensive delocalization of the electron density of iron via  $\pi$ -backbonding. Such  $\pi$ -delocalization presents an unusual reaction path for the one electron process of  $\text{RS}^-/\text{RSSR}$  interconversion. Comparisons with imidazole-DNICs find NHCs to be the "better" ligands to  $\text{Fe}(\text{NO})_2$  and prompted investigations in (a) possible relationships between such imidazole- and NHC-containing DNICs, (b) systems that might mimic the reactivity of DNICs with the endogenous gaseotransmitter CO, and (c) mechanistic details of such processes. In a broader context, these studies aim to further describe the behavior of the  $\{\text{Fe}(\text{NO})_2\}$  unit as a single molecular entity when subjected to various ligand environments and reaction conditions.



## INTRODUCTION

The simplest of ligands in a coordination chemist's toolbox, CO,  $\text{CN}^-$ , and NO, are known to play extremely important roles in biology. That their fundamental bonding abilities range from strong to weak and from spectators to "non-innocent" redox assistants of metals is consistent with nature's amazing ability to manipulate common molecules to achieve the most sophisticated functions. Our knowledge has expanded from recognition of the effects of such diatomics as toxins to biological research of enzyme mechanisms in which CO and  $\text{CN}^-$  are deliberately added as inhibitors. As detectors of bioactive metals, the use of CO for its vibrational spectral signature and of NO as an EPR active spin label has become the fundamental basis of breakthroughs that identified their

endogenous roles as signaling and regulatory agents. Later discoveries that CO and  $\text{CN}^-$  were biosynthesized in a highly controlled fashion for the purpose of building the hydrogenase ( $\text{H}_2$ ase) enzyme active sites came as a profound (and delightful) surprise to biochemists and organometallic chemists alike.<sup>1</sup>

The pyramidal  $\text{Fe}(\text{CO})(\text{CN})_2$  unit of the [NiFe]- $\text{H}_2$ ase active site and the diiron unit within the  $\text{H}_2$ -producing H-cluster of the [FeFe]- $\text{H}_2$ ase active site have inspired synthetic modifications of readily accessible small molecule mimics.<sup>6</sup> An isoelectronic analogue of the pyramidal  $[\text{Fe}^{\text{II}}(\text{CO})(\text{CN})_2]$  or

Received: April 17, 2015

Published: June 19, 2015

$\text{Fe}^{\text{I}}(\text{CO})_3$  units, the redox active dinitrosyl iron units (DNIUs)  $[\text{Fe}(\text{NO})_2]_0$  or  $[\text{Fe}(\text{NO})_2]^+$ , were early described as possibilities for building biomimetics of  $\text{H}_2$ ase active sites (Figure 1).<sup>5,7</sup> While the first report of a  $[\text{NiFe}]$ - $\text{H}_2$ ase active site

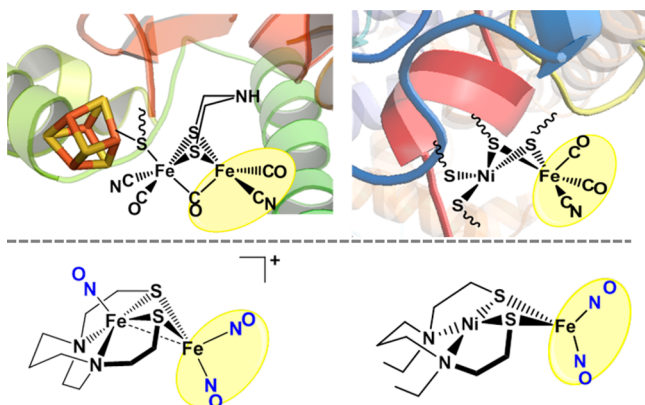


**Figure 1.** (top) Depictions (generated using PyMOL) of active sites of  $[\text{FeFe}]$ - $\text{H}_2$ ase<sup>2</sup> and  $[\text{NiFe}]$ - $\text{H}_2$ ase.<sup>3</sup> (bottom) Corresponding  $\text{Fe}(\text{NO})_2$ -containing model compounds.<sup>4,5</sup>

model making use of such a dinitrosyliron unit saw no catalytic activity, a recent one purportedly mimicking features of the  $[\text{FeFe}]$ - $\text{H}_2$ ase catalytic site is a modest catalyst for proton reduction (Figure 1).<sup>4</sup> The latter takes advantage of the two redox levels of DNIUs, described in Figure 2 according to the Enemark–Feltham electron counting scheme<sup>8</sup> and also by the oxidation state approach of Ye and Neese.<sup>9</sup>

	Oxidized $\{\text{Fe}(\text{NO})_2\}^9$						Reduced $\{\text{Fe}(\text{NO})_2\}^{10}$		
	$\text{Fe}^{\text{III}}(\text{NO})(\text{NO}) \longleftrightarrow \text{Fe}^{\text{II}}(\text{NO})(\text{NO})$						$\text{Fe}^{\text{II}}(\text{NO})(\text{NO})$		
S =	5/2	1	1	2	1/2	1	2	1	1
	2			3/2			2		
S =	1/2			1/2			0		

**Figure 2.** Correlation of valence electron count (Enemark–Feltham approach<sup>8</sup>) with Ye and Neese<sup>9</sup> analysis of oxidation states in oxidized and reduced DNIUs.

The notable ability of the DNIU to exist as an intact organometallic entity in biology is revealed by the existence of four-coordinate tetrahedral dinitrosyl iron complexes (DNICs), first identified by a characteristic EPR signal at  $g_{\text{avg}} = 2.03$ , readily related to dithiolates,  $(\text{RS})_2\text{Fe}(\text{NO})_2$ .<sup>10</sup> Derived from the action of nitric oxide on the cellular, chelatable iron pool<sup>11</sup> or by NO degradation of iron sulfur clusters,<sup>12</sup> it has been suggested that there exists equilibria between intracellular protein-bound DNICs and low molecular weight forms, the latter composed of amino acid or small peptide-complexed DNIUs.<sup>13</sup> As a highly reactive radical, free NO has a short life span of 2 ms to 2 s.<sup>14</sup> Stabilization for NO transport and storage *in vivo* is presumed to need small biomolecule-complexed entities. Studies involving the multidrug resistance protein 1 (MRP1) and the glutathione-S-transferase group of enzymes have reported that DNICs are involved in the transport and storage of endogenous NO.<sup>14</sup> This suggestion is supported by a protein crystal structure of the glutathione-S-

transferase enzyme containing  $\text{Fe}(\text{NO})_2$ , provided to the transferase in the form of a diglutathione complex, imbedded within the glutathione-binding site (Figure 3).<sup>15</sup>

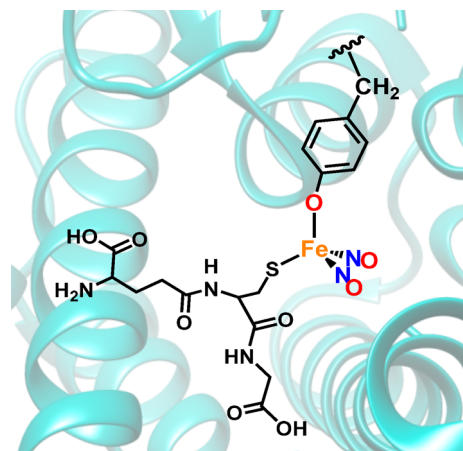


**Figure 3.** Glutathione-DNIC trapped within the active site of glutathione transferase.<sup>15</sup> Figure generated using UCSF Chimera.

Despite the extensive literature devoted to the chemistry and biochemistry of DNICs,<sup>16,17,10</sup> the fundamental features that control redox level interconversion of the intact  $\text{Fe}(\text{NO})_2$  unit or NO release in biologically relevant ligating environments remain incompletely defined. We have employed two main types of unique ligand sets that are able to impart stability on the resulting dinitrosyl iron complexes (DNICs):  $\text{MN}_2\text{S}_2$  and N-heterocyclic carbene (NHC) ligands. The former has enabled us to exploit the redox versatility of the DNIU in models of hydrogenase active site mimics. The NHC ligands have been used as analogues of histidine, offering stable models of the biological N-bound, neutral ligands. Intrigued by the integrity of the unique DNIU and the possibility of roles for it in human physiology or medicinal applications, our studies target the understanding of fundamental properties of this significant bio-organometallic entity as revealed through biomimetic complexes.

## ■ METALLODITHIOLATE LIGANDS TO $\text{Fe}(\text{NO})_2$

The stabilization of  $\text{Fe}(\text{NO})_2$  in its two redox levels by identical donors has been accommodated by only a few ligands.<sup>17,18</sup> The metallodithiolates used by us involve a contiguous arrangement of nitrogen and sulfur donor sites that mimic the Cys-Gly-Cys or Cys-Ser-Cys peptide motifs and thiolate-S/amido-N “backbone” binding sites.<sup>19,20</sup> Such  $\text{N}_2\text{S}_2$  sites, for which extensive literature is available, are known to ligate  $\text{Ni}^{2+}$ , iron (as  $\text{Fe}(\text{NO})^{2+}$  or by the Enemark–Feltham notation<sup>8</sup>  $\{\text{Fe}(\text{NO})\}^7$ ), and cobalt (as  $\text{Co}(\text{NO})^{2+}$ , or  $\{\text{Co}(\text{NO})\}^8$ ) within a largely planar  $\text{N}_2\text{S}_2$  binding pocket.<sup>21</sup> The *cis*-dithiolate sulfurs have available lone pairs that are well oriented to further serve as mono- or bidentate ligands to exogenous metals and in fact can control aggregation of up to four exogenous metals per  $\text{MN}_2\text{S}_2$ .<sup>21</sup> The versatility of such metallodithiolate ligands has been demonstrated in the formation of a variety of heterometallic, S-bridged structures, including those in which the  $\text{Fe}(\text{NO})_2$  unit has produced heterobimetallic NiFe and heterotrimetallic NiFe<sub>2</sub> complexes as well as higher order neutral, adamantyl cage clusters.<sup>21,22</sup> This collection of complexes has indicated an intricate interplay of DNIU redox

levels and the stability of the  $\text{MN}_2\text{S}_2$  donor/ $\text{Fe}(\text{NO})_2$  acceptor adducts.

We focus on diazacycles as frameworks for attachment of mercaptoethane arms that yield stable, readily modifiable, neutral  $\text{MN}_2\text{S}_2$  metalloligands. Table 1 lists examples of DNICs in two redox levels; the first four entries, **1**, **2**, **3<sup>+</sup>**, and **4**, contain  $\{\text{Fe}(\text{NO})_2\}^9$  with traditional ligands as well as the NHC and  $\text{MN}_2\text{S}_2$  ligands. The second group, **5–8** and **3**, are  $\{\text{Fe}(\text{NO})_2\}^{10}$  derivatives. The sensitivity of  $\nu(\text{NO})$  to ligand effects on the Fe is clearly seen in the successive replacement of CO by the good electron-donating NHC ligands, entries **5–7**.

**Table 1.** Selected  $\{\text{Fe}(\text{NO})_2\}$  Complexes Containing NHC/ $\text{MN}_2\text{S}_2$  Ligands

	$\{\text{Fe}(\text{NO})_2\}^9$	$\nu(\text{NO})$ ( $\text{cm}^{-1}$ ) <sup>a</sup>
<b>1</b> <sup>23</sup>		1709, 1744
<b>2</b> <sup>7</sup>		1725, 1767, (1805)
<b>3</b> <sup>3+</sup>		1742, 1796 (1761)
<b>4</b> <sup>24</sup>		1712, 1757
	$\{\text{Fe}(\text{NO})_2\}^{10}$	$\nu(\text{NO})$ ( $\text{cm}^{-1}$ ) <sup>a</sup>
<b>5</b> <sup>25</sup>		1756, 1810 (2034, 2087)
<b>6</b> <sup>24</sup>		1696, 1738 (1988)
<b>7</b> <sup>24</sup>		1619, 1664
<b>8</b> <sup>7</sup>		1630, 1677
<b>3</b> <sup>4</sup>		1640, 1690 (1662)

<sup>a</sup> $\nu(\text{NO})$  data for the  $\text{Fe}(\text{NO})_2$  unit with  $\nu(\text{NO})$  or  $\nu(\text{CO})$  of additional diatomic in parentheses.

Similarly, in the oxidized regime, the  $\nu(\text{NO})$  in  $\{\text{Fe}(\text{NO})_2\}^9$  responds as expected in complexes **1** and **4**. Such regular responses within the redox levels are critical in classifying the metallodithiolates as ligands.

Entries **3<sup>+</sup>** and **3** of Table 1 are examples of identical formulations of  $\text{MN}_2\text{S}_2\cdot\text{Fe}(\text{NO})_2$  in two redox levels. Electrochemical and spectroscopic (EPR data) data and DFT computations suggest that the reduction of **3<sup>+</sup>** to **3** involves localizing the added electron to the DNIU, generating  $\{\text{Fe}(\text{NO})_2\}^{10}$ .<sup>4</sup> The  $\nu(\text{NO})$  report of electron densities and  $\pi$  backbonding from the  $\text{Fe}(\text{NO})_2$  units find a ca.  $100\text{ cm}^{-1}$  shift to lower values in the  $\{\text{Fe}(\text{NO})_2\}^9$  to  $\{\text{Fe}(\text{NO})_2\}^{10}$  reduction.<sup>4</sup> In addition, the  $\nu(\text{NO})$  values of the  $\{\text{Fe}(\text{NO})\}^7$  unit imbedded in the  $\text{N}_2\text{S}_2$  binding pocket is also displaced by ca.  $100\text{ cm}^{-1}$  to lower values, approaching the  $\nu(\text{NO})$  value of the free  $\text{N}_2\text{S}_2\text{Fe}(\text{NO})$  ligand, implying that less electron density is drained from the  $\{\text{Fe}(\text{NO})\}^7$  by  $\{\text{Fe}(\text{NO})_2\}^{10}$  compared with the  $\{\text{Fe}(\text{NO})_2\}^9$  acceptor. Complex **3** is very air and thermally sensitive, in strong contrast to the stability of the oxidized complex **3<sup>+</sup>**. In fact, several reactions have found the  $\text{Fe}_2(\text{NO})_3^+$  motif of **3<sup>+</sup>** to be a common, sometimes unexpected, byproduct, reflecting its thermodynamic stability, *vide infra*. Interestingly, the oxidized analogue of complex **8** cannot be isolated, despite the ranking of the  $\text{Ni}(\text{bme-daco})$  ligand as a better electron donor than the  $\text{Fe}(\text{NO})(\text{bme-daco})$  dithiolate ligand, which was expected to better stabilize  $\{\text{Fe}(\text{NO})_2\}^9$ .

#### THE $[\text{Fe}(\text{NO})\text{N}_2\text{S}_2\cdot\text{Fe}(\text{NO})_2]^+$ COMPLEX, **3<sup>+</sup>**, AS ELECTROCATALYST FOR $\text{H}^+$ REDUCTION

The possibility that  $\text{MN}_2\text{S}_2\cdot\text{Fe}(\text{NO})_2$  complexes might serve as functional models of hydrogenase active sites was realized in complex **3<sup>+</sup>**. Reversible waves in the cyclic voltammogram are assigned to the individual redox active units,  $\{\text{Fe}(\text{NO})_2\}^{9/10}$  and  $\{\text{Fe}(\text{NO})\}^{7/8}$ , at  $-0.78$  and  $-1.41\text{ V}$  (referenced to  $\text{Fc}/\text{Fc}^+$  couple), respectively (Figure 4). These assignments, consistent with comparisons of monomeric counterparts, were supported by theory and spectroscopy. For example, the EPR spectrum of the one-electron reduced **3<sup>+</sup>**, that is, complex **3**, well matched

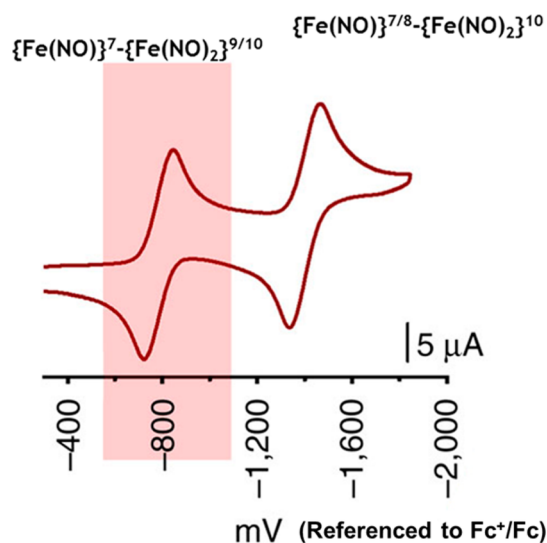


**Figure 4.** Cyclic voltammogram of **3<sup>+</sup>** with the first wave highlighted. Scan rate is  $200\text{ mV/s}$ ,  $2\text{ mM CH}_2\text{Cl}_2$  solutions of **3<sup>+</sup>** under Ar, referenced to  $\text{Fc}^+/\text{Fc}$ .<sup>4</sup>

that of the  $\{\text{Fe}(\text{NO})\}^7$  in monomeric,  $S = 1/2$ ,  $(\text{NO})\text{Fe}(\text{N}_2\text{S}_2)^4$ .

The more positive event in the cyclic voltammogram of complex  $3^+/3$  was found to have a linear response to added equivalents of the  $\text{HBF}_4$  acid (Figure 5), and analysis of the gas

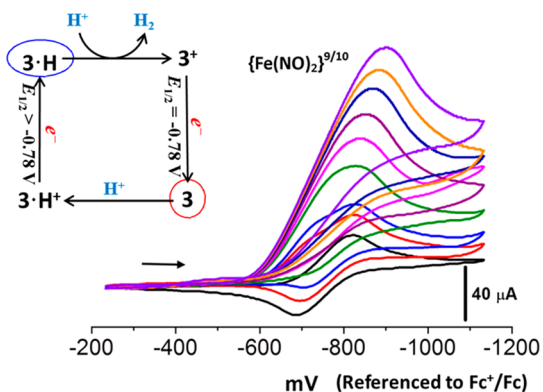


**Figure 5.** Electrochemical response of complex  $3^+$  in  $\text{CH}_2\text{Cl}_2$  solution to added equivalents of  $\text{HBF}_4$  (8 equiv range; 0 (black line) to 8 (blue line) at the first reduction event ( $-0.78$  V), where  $3$  is the product, referenced to  $\text{Fc}^+/\text{Fc}$ .<sup>4</sup>

produced from bulk electrolysis identified  $\text{H}_2$  as product.<sup>4</sup> Computational approaches (DFT) to the mechanism found multiple sites for electron delocalization and protonation. Although turnover numbers and catalytic efficiency for the  $3^+$  reduction/protonation cycle were poor, the proof of principle provided by this molecular platform encourages studies in catalyst optimization.

## ■ SYNTHETIC APPROACHES TO THE $\text{MN}_2\text{S}_2\text{Fe}(\text{NO})_2$ PLATFORMS

Figure 6 displays synthetic routes to several DNICs making use of the reduced  $\text{Fe}(\text{CO})_2(\text{NO})_2$  synthon, especially for the  $\text{MN}_2\text{S}_2\text{Fe}(\text{NO})_2$  derivatives. Simple mixing with  $\text{Ni}(\text{bme-dach})$  yields the  $\text{NiN}_2\text{S}_2\text{Fe}(\text{NO})_2(\text{CO})$  complex, replacing

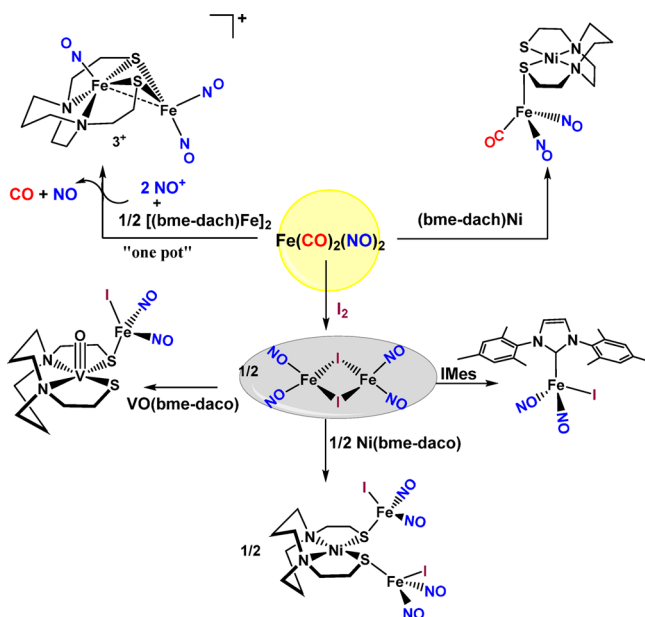


**Figure 6.** Synthetic routes via the  $\text{Fe}(\text{CO})_2(\text{NO})_2$  synthon.

only one CO with  $\text{NiN}_2\text{S}_2$  in a monodentate binding mode.<sup>26</sup> A “one-pot” mixture of the  $[\text{Fe}(\text{bme-dach})]_2/\text{Fe}(\text{CO})_2(\text{NO})_2$  with  $\text{NO}^+$  leads to loss of CO with formation of complex  $3^+$ .<sup>4</sup> Addition of  $\text{I}_2$  to  $\text{Fe}(\text{CO})_2(\text{NO})_2$  generates the iodide-bridged, oxidized  $\{\text{Fe}(\text{NO})_2\}^9$  dimer, which itself can be used to generate  $\text{Fe}(\text{NO})_2\text{I}$  derivatives of the NHC, the vanadyl- $\text{N}_2\text{S}_2$ , or the  $\text{NiN}_2\text{S}_2$  metalloligand, Figure 6.<sup>27</sup> Notably, the  $(\mu\text{-I})_2[\text{Fe}(\text{NO})_2]_2$  dimer<sup>28</sup> is the analogue of the so-called “Roussin’s red ester” (RRE),  $(\mu\text{-RS})_2[\text{Fe}(\text{NO})_2]_2$ ,<sup>29</sup> described later as a useful synthon for thiolate-containing DNICs.

An especially useful synthon for the preparation of  $\text{MN}_2\text{S}_2$ -DNIC derivatives has been the NHC trinitrosyl iron complex, a TNIC, shown in Figure 7 (and further discussed later).

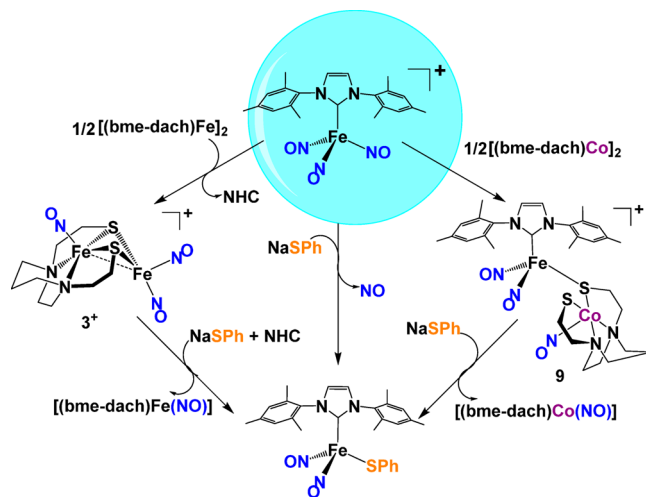


**Figure 7.** Synthetic routes via the NHC trinitrosyl iron complex.

Addition of dimeric  $[(\text{bme-dach})\text{M}]_2$ ,  $\text{M} = \text{Co}$  and  $\text{Fe}$ , results in NO transfer to the metals of the dimers with subsequent loss of the NHC in the case of  $\text{Fe}$ , generating the very stable complex  $3^+$ .<sup>30</sup> For  $\text{M} = \text{Co}$ , known to be an even better scavenger of NO than the  $\text{Fe}$  complex, the  $\text{Co}(\text{NO})\text{N}_2\text{S}_2$  metallothiolate produces monodentate S-binding (complex 9), as shown in Figure 7.<sup>31</sup> The reason why the displacement of the NHC is not favored for this metallodithiolate ligand is not clear, because it has been established to have almost identical spectroscopic and electrochemical properties as its iron analogue, with the exception that the  $\{\text{Fe}(\text{NO})\}^9$  unit is paramagnetic,  $S = 1/2$ , while the  $\{\text{Co}(\text{NO})\}^{10}$ , reasonably formulated as a  $\text{Co}^{\text{III}}(\text{NO}^-)$  unit, is diamagnetic.

## ■ A BIOMIMETIC DESIGN

The ability of the  $\text{N}_2\text{S}_2$  ligand to sequester  $\text{Fe}(\text{NO})$  was used to advantage in the exploration of NO release from  $\{\text{Fe}(\text{NO})_2\}^9$ . As a biomimetic for protein-bound  $\text{Fe}(\text{NO})_2$ , the protonated  $\text{bme-daco}$  ligand, with two anionic thiolates available for bonding, was used as an analogue of the sulfurs in  $-\text{Cys-X}_n-\text{Cys}$  motifs that are expected to account for Vanin’s hypothesis<sup>13</sup> for a protein-bound, high molecular weight DNIC, Figure 8. The  $(\text{H}^+\text{-bme-daco})\text{Fe}(\text{NO})_2$  complex 10, prepared from the reaction of the free ligand as a dithiol with  $[\text{I}_2\text{Fe}(\text{NO})_2]^-$ , was isolated and crystallized at low temperatures, and its structure was determined by X-ray diffraction.<sup>32</sup> Solution studies found that in the presence of a NO acceptor such as an iron porphyrin, serving as a model for the active site of soluble guanylyl cyclase (a primary target of NO in cells), a NO

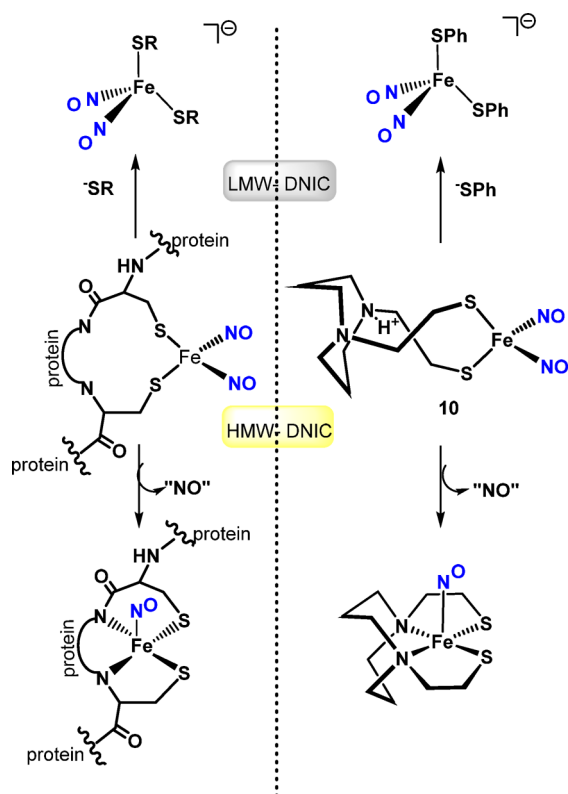


**Figure 8.** (right panel) The  $(\text{H}^+\text{-bme-daco})\text{Fe}(\text{NO})_2$  complex as a biomimetic for protein-bound  $\text{Fe}(\text{NO})_2$ . (left panel) Proposed analogous biochemical process.<sup>32,33</sup>

was removed from the DNIC. As indicated in Figure 8, the remaining  $\text{Fe}(\text{NO})$  slipped into the  $\text{N}_2\text{S}_2$  binding site, forming the highly stable  $\text{Fe}(\text{NO})\text{N}_2\text{S}_2$ .<sup>32,33</sup> To our knowledge, the analogous biochemical process expressed in Figure 8 (left panel), that is, the formation of the mononitrosyl derivative as a product concurrent with NO transfer, has not been proposed by others. As the signature EPR signal of the  $\text{Cys-X}_n\text{-Cys-Fe}(\text{NO})$  is expected to be the same as the small molecule  $\{\text{Fe}(\text{NO})\}^7$  model,  $g = 2.05$ , such similarity to the characteristic  $\{\text{Fe}(\text{NO})_2\}^9$  signal of  $g = 2.03$  might have prevented its discovery.

The  $(\text{H}^+\text{-bme-daco})\text{Fe}(\text{NO})_2$  complex **10** also served to model transfer of the intact  $\text{Fe}(\text{NO})_2$  unit from the protein bound, high molecular weight DNIC, to a mobile, low molecular weight form, LMW-DNIC, Figure 8. In the presence of  $\text{PhS}^-$  as a mimic of thiolates from free cysteine or glutathione, the  $(\text{PhS})_2\text{Fe}(\text{NO})_2^-$  was obtained within time of mixing.<sup>32</sup>

### ■ MONOMERIC SYNTHETIC MODELS OF HISTIDINE BOUND BIOLOGICAL DNICS

Typical biological DNICs are of the  $\text{X}_2\text{Fe}(\text{NO})_2^-$ ,  $\{\text{Fe}(\text{NO})_2\}^9$  type, where X = cysteine or glutathione thiolate S-donors; synthetic models have also commonly been based on thiolate ligands, as seen in monomeric, paramagnetic  $(\text{RS})_2\text{Fe}(\text{NO})_2^-$ , as well as the dimeric, diamagnetic  $(\mu\text{-RS})_2[\text{Fe}(\text{NO})_2]_2$ ,<sup>16</sup> where the  $\{\text{Fe}(\text{NO})_2\}^9$  units of the latter are spin coupled ( $\text{Fe}\cdots\text{Fe} \approx 2.7 \text{ \AA}$ ).<sup>34</sup> The DNICs containing N-donor ligand sets, primarily of the neutral  $\text{L}_2\text{Fe}(\text{NO})_2$  ( $\{\text{Fe}(\text{NO})_2\}^{10}$ ) and  $\text{L}(\text{X})\text{Fe}(\text{NO})_2$  ( $\{\text{Fe}(\text{NO})_2\}^9$ ) types are of interest because such ligands mimic the coordination of histidine to  $\text{Fe}(\text{NO})_2$ . While

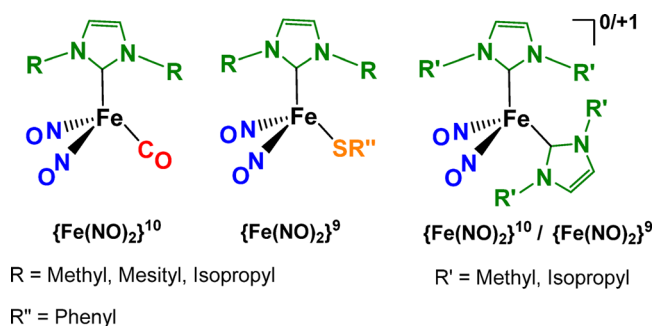
cysteine coordination can be considered as a straightforward thiolate ligand binding, histidine coordination to metals is relatively more complex due the possibility of two N-binding sites: a nitrogen base and a second imidazole amine nitrogen that can be deprotonated.

Li et al. prepared a series of six imidazole-DNICs as surrogates of histidine-DNICs by reaction with  $\text{Fe}(\text{CO})_2(\text{NO})_2$ , the common starting precursor for  $\{\text{Fe}(\text{NO})_2\}^{10}$  DNICs.<sup>35,36</sup> Within the series, only  $\text{Fe}(\text{NO})_2(1\text{-MeIm})_2$  (1-MeIm = 1-methyl imidazole) could be isolated and characterized in its reduced,  $\{\text{Fe}(\text{NO})_2\}^{10}$ , form.<sup>35</sup> All derivatives were found to have in solution EPR signals with a  $g$  value of ca. 2.03, indicative of the formation of the oxidized species. Therefore, this study revealed that despite its obvious structural similarity to histidine, imidazole and its derivatives had limited success at stabilizing reduced DNICs.

The versatile and extremely useful N-heterocyclic carbenes are synthesized by deprotonation of the appropriate imidazolium salts.<sup>37,38</sup> One of our studies, driven by the presence of histidine donors in binding sites of Ni-containing biomolecules, explored orientational preferences of such monodentate, flat ligands as imidazoles and NHCs bound to planar  $[\text{N}_2\text{S}\text{Ni}^+]$  moieties, finding no significant differences in metric parameters and the orientation of the plane of the ligand with respect to the  $\text{N}_2\text{S}\text{Ni}$  plane.<sup>39</sup> Such fortunate correlations between imidazoles and NHCs prompted us to investigate the suitability of NHC ligands in the synthesis of stable model DNICs in different redox levels and reactivity studies thereof.

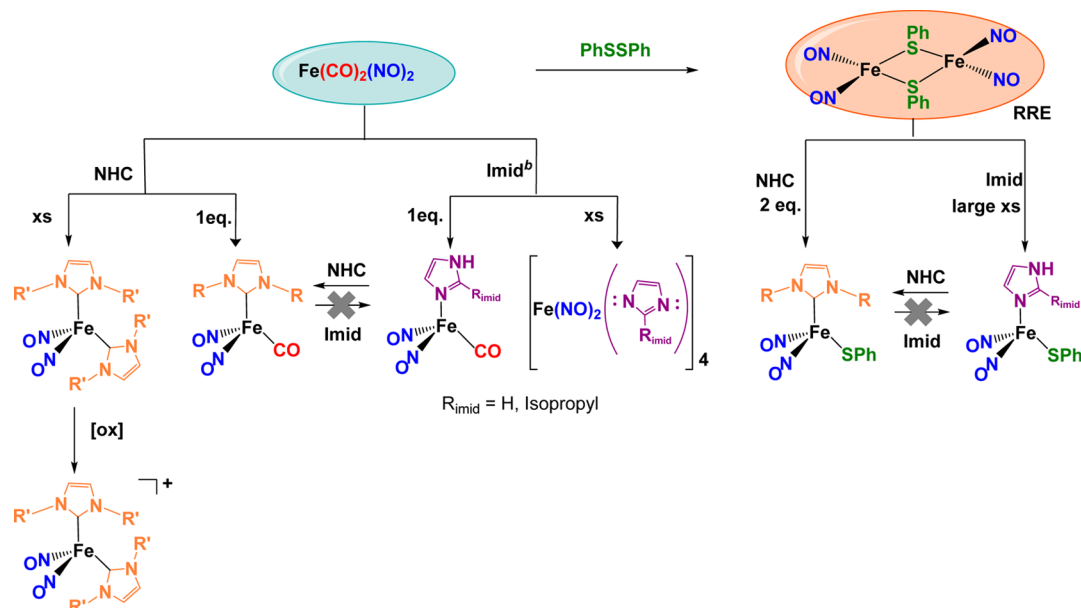
### ■ A NEW FAMILY OF N-HETEROCYCLIC CARBENE STABILIZED MONOMERIC DNICS

Explorations of the suitability of NHC ligands to stabilize the  $\{\text{Fe}(\text{NO})_2\}^9$  and  $\{\text{Fe}(\text{NO})_2\}^{10}$  redox levels of DNICs has mainly been based on the prototypes shown in Figure 9.



**Figure 9.** Prototypic NHC-DNICs in two redox levels.

Scheme 1 summarizes the synthetic design. Among these, the neutral  $\{\text{Fe}(\text{NO})_2\}^{10}$  compounds are of the  $\text{L}_2\text{Fe}(\text{NO})_2$  type and can be accessed readily through CO/L ligand exchange for  $\text{L} = \text{NHC}$  and precursor  $\text{Fe}(\text{CO})_2(\text{NO})_2$ . The mono- and bis-NHC-substituted, reduced DNICs can be obtained in this way via appropriate stoichiometric control (the steric constraints of bulky NHC ligands such as IMes prevent disubstitution).<sup>24</sup> The cleavage of dimeric  $(\mu\text{-RS})_2[\text{Fe}(\text{NO})_2]_2$ , with the relevant NHC results in stoichiometric conversion of the RRE to neutral, oxidized  $\text{L}(\text{X})\text{Fe}(\text{NO})_2$  type DNICs. While this is the more clearly defined route to oxidized, NHC-bearing DNICs, the reaction of neutral bis-NHC DNICs with oxidants such as  $\text{O}_2$  and  $\text{NO}^+$  also results in the formation of  $\text{L}_2\text{Fe}(\text{NO})_2^+$ ,  $\{\text{Fe}(\text{NO})_2\}^9$  compounds.<sup>24</sup>

Scheme 1. Synthetic Approaches<sup>a</sup>

<sup>a</sup>Refer to Figure 9 for identity of R and R'. <sup>b</sup>The imidazoles shown as well as benzimidazole have been used.

For comparison to NHC-DNICs, the analogous imidazole bound DNICs were prepared (Scheme 1). The monosubstituted  $\{\text{Fe}(\text{NO})_2\}^{10}$  complex was obtained using 1 equiv of imidazole; however, contrary to the NHCs, addition of excess imidazole resulted in the formation of interesting imidazolate-bridged, tetrameric  $[(\text{Imid})\text{Fe}(\text{NO})_2]_4$  complexes<sup>24,40</sup> with  $\{\text{Fe}(\text{NO})_2\}^9$  units surprisingly similar to  $[(\text{Imid})\text{Cu}(\text{tacn})]_4^{4+}$  molecular squares (Figure 10).<sup>41</sup> Imidazoles could also cleave

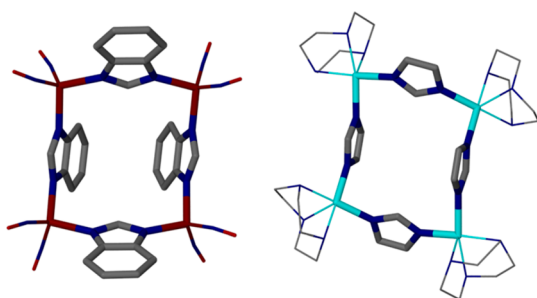


**Figure 10.** Capped stick renditions of (left)  $[(\text{Imid-benz})\text{Fe}(\text{NO})_2]_4$  and (right)  $[(\text{Imid})\text{Cu}(\text{tacn})]_4^{4+}$  molecular squares.<sup>40,41</sup>

the RRE to yield the monosubstituted  $\{\text{Fe}(\text{NO})_2\}^9$  compound as can NHCs. However, unlike the NHCs, the complete conversion of the RRE required a large excess of (>14 equiv) imidazole.

## STRUCTURAL AND SPECTROSCOPIC STANDARDS

All monomeric DNICs containing NHC ligands are four coordinate, pseudotetrahedral compounds with average  $\angle\text{C}-\text{Fe}-\text{NO}$  angles in the range of  $106-110^\circ$ . The  $\angle\text{N}-\text{Fe}-\text{N}$  values range from  $110.9^\circ$  to  $121.9^\circ$ , with the reduced compounds at the larger end of the range.<sup>24,30,42-44</sup> These values compare well with the metrics of Li's bis-imidazole DNIC,  $(\text{Imid-Me})_2\text{Fe}(\text{NO})_2$ , in which the  $\angle\text{N}_{\text{imid}}-\text{Fe}-\text{NO}$  averages ca.  $112.0^\circ$  and the  $\angle\text{N}-\text{Fe}-\text{N}$  is  $116.6^\circ$ .<sup>35</sup> The  $\text{Fe}-\text{N}-\text{O}$  angles in the NHC-DNICs are largely linear with the reduced forms averaging to  $174^\circ$  and the oxidized forms slightly less (ca.  $168^\circ$ ). The bis-imidazole complex  $(\text{Imid-Me})_2\text{Fe}(\text{NO})_2$  also has  $\angle_{\text{avg}}(\text{Fe}-\text{N}-\text{O}) = 168^\circ$ . In both the oxidized and reduced NHC-DNICs, deviation from linearity is in the form of the NO ligands bending symmetrically toward each other within the coplanar  $\text{Fe}(\text{NO})_2$  unit. Interestingly, such an "attracto" orientation<sup>8,45,46</sup> is maintained in bimetallics and clusters that were previously discussed.

The IR stretching frequencies of the diatomic ligands such as NO and CO in selected monomeric DNICs are shown in Table 1. Extensive compilations of  $\nu(\text{NO})$  values, of which Table 1 is a subset, find that  $\nu(\text{NO})$  values that define the  $\{\text{Fe}(\text{NO})_2\}^{10}$  NHC-DNICs are in the  $1620-1750\text{ cm}^{-1}$  range, shifting to much more positive values, from  $1710$  to  $1790\text{ cm}^{-1}$ , in the oxidized  $\{\text{Fe}(\text{NO})_2\}^9$  form.<sup>24,30,42-44</sup> Back-bonding arguments account for these results, which are also consistent with metric

**Table 2.** Mössbauer Parameters and  $\nu(\text{NO})$  Values of Selected DNICs

	redox level	$\delta$ (mm/s)	$\Delta E_Q$ (mm/s)	$\nu(\text{NO})$ ( $\text{cm}^{-1}$ )	ref
$[(\text{NHC-}i\text{Pr})_2\text{Fe}(\text{NO})_2]^0$	$\{\text{Fe}(\text{NO})_2\}^{10}$	0.045	1.34	1619, 1664	40
$[(\text{NHC-}i\text{Pr})_2\text{Fe}(\text{NO})_2]^+$	$\{\text{Fe}(\text{NO})_2\}^9$	0.114	0.265	1723, 1791	40
$[(\text{Ar-nacnac})\text{Fe}(\text{NO})_2]^{1-}$	$\{\text{Fe}(\text{NO})_2\}^{10}$	0.22	1.31	1567, 1627	18
$[(\text{Ar-nacnac})\text{Fe}(\text{NO})_2]^0$	$\{\text{Fe}(\text{NO})_2\}^9$	0.19	0.79	1709, 1761	18
$[(\text{NHC-}i\text{Pr})(\text{CO})\text{Fe}(\text{NO})_2]$	$\{\text{Fe}(\text{NO})_2\}^{10}$	0.022	0.818	1696, 1738	40
$[(\text{NHC-}i\text{Pr})(\text{SPh})\text{Fe}(\text{NO})_2]$	$\{\text{Fe}(\text{NO})_2\}^9$	0.151	0.513	1712, 1757	40
$[\text{Fe}(\text{CO})_2(\text{NO})_2]$	$\{\text{Fe}(\text{NO})_2\}^{10}$	0.027	0.332	1807, 1762	40, 24

data. As with four-coordinate DNICs containing ligands other than NHCs,<sup>16</sup>  $\Delta\nu_{\text{NO}}$  ( $\Delta\nu_{\text{NO}}$  = the difference between the  $\nu(\text{NO})$  band positions) falls into the range around 40–60  $\text{cm}^{-1}$ . Although quite similar, the IR stretching frequencies for the imidazole-containing DNIC counterparts of the NHCs imply that the latter are the better donors.

The presence of the notoriously noninnocent NO ligands gives rise to ambiguity in the assignment of oxidation states to the iron center of DNICs, which Mössbauer data might be expected to resolve. However, Lippard's reduced and oxidized  $[(\text{Ar-nacnac})\text{Fe}(\text{NO})_2]^{-/0}$  complexes ( $[(2,6\text{-diisopropylphenyl})\text{NC}(\text{Me})_2\text{CH} = (\text{Ar-nacnac})]$ ) were reported to have similar isomer shift values (Table 2).<sup>18</sup> According to the computational studies on this system by Ye and Neese,<sup>9</sup> the  $\{\text{Fe}(\text{NO})_2\}$  unit is best described by two resonance structures: a high spin-Fe(III) (HS-Fe(III)),  $d^5$  antiferromagnetically coupled to two triplet  $\text{NO}^-$  ligands and a HS-Fe(II),  $d^6$  antiferromagnetically coupled to an overall quartet from two  $\text{NO}^-$  ligands, see Figure 2. The  $\{\text{Fe}(\text{NO})_2\}^{10}$  species is described as a HS-Fe(II) center,  $S = 2$ , antiferromagnetically coupled to two triplet  $\text{NO}^-$  ligands. Computations further find that counteracting forces of oxidation state of the metal and backbonding abilities of the ligands result in the similar isomer shift values.<sup>9</sup>

In contrast to Lippard's (Ar-nacnac)-DNICs, the Mössbauer spectroscopic parameters of the prototypic NHC-DNICs in Figure 9 show that the oxidized  $\{\text{Fe}(\text{NO})_2\}^9$  complexes have larger positive isomer shifts than the reduced  $\{\text{Fe}(\text{NO})_2\}^{10}$  analogues (Table 2).<sup>40</sup> For example, the isomer shift of the reduced DNIC  $[(\text{NHC-iPr})(\text{CO})\text{Fe}(\text{NO})_2]$ , 0.022 mm/s, is consistent with recorded data for  $(\text{Ph}_3\text{P})(\text{CO})\text{Fe}(\text{NO})_2$  and  $(\text{Ph}_3\text{P})_2\text{Fe}(\text{NO})_2$ . In contrast, the oxidized DNIC  $[(\text{NHC-iPr})(\text{SPh})\text{Fe}(\text{NO})_2]$  has an isomer shift of 0.151 mm/s, matching that of the analogous  $\{\text{Fe}(\text{NO})_2\}^9$  complex,  $[(\text{PhS})_2\text{Fe}(\text{NO})_2]^-$ ,  $\delta = 0.18$  mm/s. The lower isomer shifts of the reduced compounds (containing CO in place of a  $^-$ SPh in the above example), are indicative of greater delocalization of the electron density of iron via  $\pi$ -backbonding.<sup>40</sup>

These studies involving structural and spectroscopic characterization of the series of NHC-DNICs confirmed the suitability of NHC ligands as mimics of imidazole/histidine in stable model DNICs of different redox levels. A fundamental expectation, experimentally observed, is that the Fe–NO bond should be stronger in the reduced complexes and NO release is favored in the oxidized  $\{\text{Fe}(\text{NO})_2\}^9$  form.<sup>24,30</sup>

### ■ ESTABLISHING CORRELATIONS IN REACTIVITY PATTERNS BETWEEN NHC-DNICs AND IMIDAZOLE-DNICs

Reactivity studies involving NHC-DNICs and Imid-DNICs, Scheme 1, showed that while NHCs were capable of readily displacing imidazoles from both the oxidized (Imid-R)(SPh)- $\text{Fe}(\text{NO})_2$  and the reduced (Imid-R)(CO) $\text{Fe}(\text{NO})_2$  compound; the reverse process, that is, the displacement of NHCs by imidazole ligands on the corresponding NHC-DNICs, did not take place.<sup>24</sup> These competition studies indicated that the stronger donor NHCs appear to be “better” ligands to  $\text{Fe}(\text{NO})_2$  than imidazoles. Building on this premise, and intrigued by a DFT study by Crabtree et al. that suggested a metal dependent preference for C- vs N-binding of imidazoles,<sup>47</sup> we investigated the possibility of conversion of an imidazole to an NHC on a dinitrosyl iron scaffold.

A mesityl-imidazole bound  $\{\text{Fe}(\text{NO})_2\}^{10}$  DNIC,  $[(\text{MesitylIm})(\text{CO})\text{Fe}(\text{NO})_2]$ , was treated with a strong base as means of initiating a possible isomerization.<sup>44</sup> The changes that accompanied this process were monitored by IR spectroscopy. As shown in Figure 11, deprotonation at the

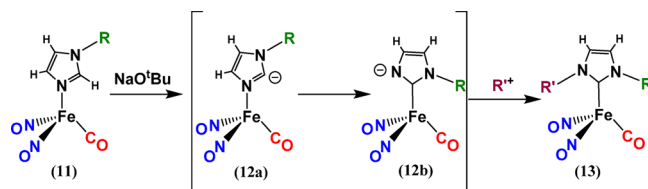


**Figure 11.** Base promoted imidazole to NHC conversion on a  $\{\text{Fe}(\text{NO})_2\}^{10}$  moiety (R = mesityl, R' = methyl, R' =  $\text{Me}_3\text{O}^+$ ).<sup>44</sup> Adapted with permission from ref 44, 2013 The Royal Society of Chemistry.

C2 position of the imidazole ring of **11** by the base resulted in the formation of unstable intermediate species, proposed as **12a/12b**. Subsequent alkylation resulted in the formation of the NHC-bound DNIC, (NHC-Me-Mes) $\text{Fe}(\text{CO})(\text{NO})_2$  (complex **13**), thereby completing the N-bound imidazole to C-bound carbene switching process. It is noteworthy that the resulting DNIC contains an asymmetric NHC, thereby suggesting this to be a possible route for such syntheses, as well as further conversion to the corresponding TNIC,  $[(\text{NHC-Me-Mes})\text{Fe}(\text{NO})_3]^+$  by isoelectronic replacement of CO by  $\text{NO}^+$ .<sup>44</sup>

This model study demonstrated the impressive stability of the dinitrosyliron unit under base treatment, while supporting the isomerization of metal-bound imidazole to an NHC ligand. To our knowledge, only a few other examples of such interconversions exist in the organometallic literature.

### ■ MIMICKING REACTIVITY OF DNICs WITH THE ENDOGENOUS GASEOTRANSMITTER<sup>48</sup> CO

We found the NHC-stabilized DNICs to be suitable for detailed studies with biologically relevant molecules; a particularly interesting case being the reactivity with CO.<sup>42</sup> Figure 12 summarizes the reaction of an NHC-stabilized  $\{\text{Fe}(\text{NO})_2\}^9$  DNIC, (sIMes)(SPh) $\text{Fe}(\text{NO})_2$ , with CO, proceeding under mild conditions and, interestingly, involving a  $\{\text{Fe}(\text{NO})_2\}^9/\{\text{Fe}(\text{NO})_2\}^{10}$  redox conversion. The process resulted in the bimolecular reductive elimination of disulfide from the oxidized thiolate DNIC, concomitant with the formation of the reduced  $\{\text{Fe}(\text{NO})_2\}^{10}$  DNIC, (sIMes)(CO)- $\text{Fe}(\text{NO})_2$ . The involvement of thiol–disulfide conversion as triggered by CO was intriguing because it could be viewed as a potential model for intracellular, thiol-complexed DNICs, exposed to intracellular CO. *In situ* IR spectroscopy permitted kinetic analysis, which suggested an overall bimolecular process. The small  $\Delta H^\ddagger$  value and large negative  $\Delta S^\ddagger$  value are indicative of an associative mechanism, consistent with the second order rate expression (Figure 12).<sup>42</sup>

Computational investigations carried out in pursuit of a possible mechanism indicated a unique role for the delocalized frontier molecular orbitals of the  $\text{Fe}(\text{NO})_2$  unit, permitting ligand exchange of  $\cdot\text{SR}$  and CO through an initial side-on approach of CO to the electron-rich N–Fe–N site (Figure 12a,b). This interaction resulted in a five-coordinate, 19-electron intermediate with an elongated Fe–SR bond, while the NO ligands bend in accommodation of the excess charge.<sup>42</sup>

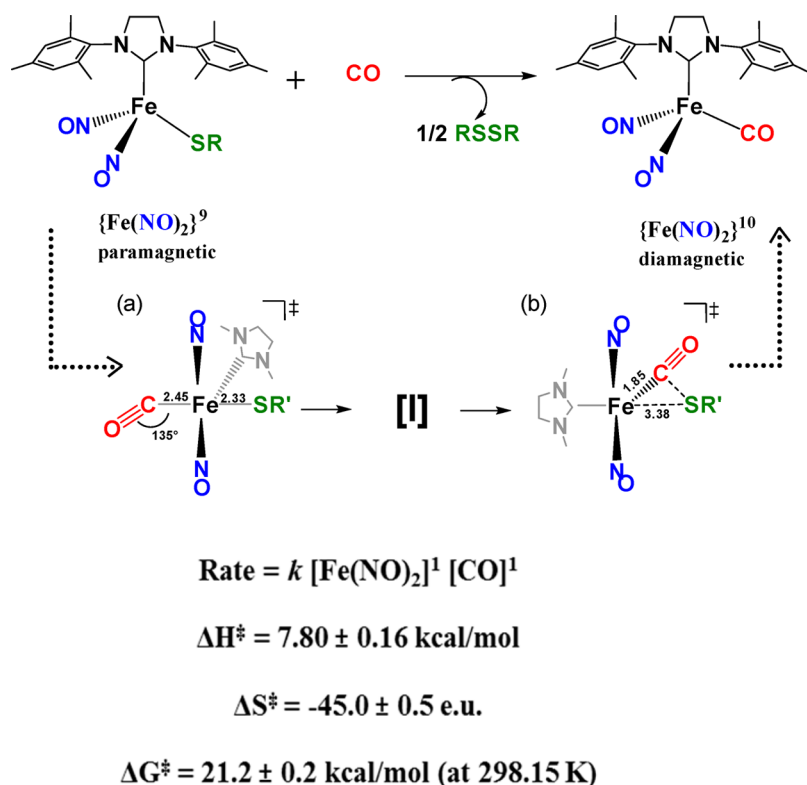


**Figure 12.** (top) CO induced elimination of disulfide in a  $\{\text{Fe}(\text{NO})_2\}^9$  NHC-DNIC ( $R = \text{Ph}$ ). (bottom) A sketch of the calculated collision complex (a,  $R' = \text{Me}$ ), involved in the rate-determining step. DFT computations find this to proceed through a five-coordinate intermediate I, to structure b, in which, as the Fe–CO bond becomes linear, the Fe–SR bond lengthens and releases a thiyl radical either by direct homolytic Fe–S bond cleavage or via homolytic C–S cleavage from a transient metallothioester group.<sup>42</sup>

In order to experimentally test the mechanistic proposal from computations,  $\{\text{Fe}(\text{NO})_2\}^9$  derivatives in the form of  $[(\text{NHC})-(p\text{-S-C}_6\text{H}_4\text{X})\text{Fe}(\text{NO})_2]$  complexes were prepared, with systematic variation of the *para*-substituents X from electron donating to electron withdrawing groups (*p*-OCH<sub>3</sub>, *p*-CH<sub>3</sub>, *p*-Cl, *p*-CF<sub>3</sub> and *p*-NO<sub>2</sub>).<sup>43</sup> Hammett analyses were carried out using infrared spectroscopic and cyclic voltammetric data as indicators of the electron density at the  $\{\text{Fe}(\text{NO})_2\}$  unit, as a result of the changes made through the aryl substituent. In a manner similar to the unsubstituted species, each derivative on reaction with CO showed conversion to the reduced (sIMes)-(CO)Fe(NO)<sub>2</sub> species, with the elimination of the corresponding substituted disulfide. Systematic changes in the rates of reaction of each derivative with CO as visualized via Hammett analyses were consistent with the electronic changes at the  $\{\text{Fe}(\text{NO})_2\}$  unit. From such data a  $\rho$  value of  $-0.831$  was obtained, indicating rate retardation by electron-withdrawing substituents. These results were in agreement with the unique role proposed in the computations for the delocalized  $\pi$  frontier molecular orbitals of the Fe(NO)<sub>2</sub>. There is loss of negative charge at the Fe(NO)<sub>2</sub> unit as a result of its initial interaction with an incoming CO molecule via the empty  $\pi^*$  orbital of CO. As an aside, the involvement of the DNIC redox couples in RS<sup>−</sup>/RSSR interconversions is mirrored by d<sup>9</sup>-Cu<sup>II</sup>/d<sup>10</sup>-Cu<sup>I</sup> couples.<sup>42</sup>

#### ■ A UNIQUE SUBSET: NHC-TRINITROSYL IRON COMPLEXES (NHC-TNICs)

Although NHC-DNICs constitute a larger component of our contribution to metal-nitrosyl complexes, success in this area stemmed from the synthesis and isolation of a trinitrosyl iron

complex, stabilized by an NHC.<sup>30</sup> Previous reports of synthetic TNICs present them as inherently thermally unstable species.<sup>49</sup> Berke et al. studied  $[(\text{R}_3\text{P})\text{Fe}(\text{NO})_3]^+$  compounds in the context of nitric oxide releasing prodrugs; however the overly rapid release of NO would be a drawback in the intended application as prodrugs.<sup>50</sup> A superior possibility, the  $[(\text{NHC-Mes})\text{Fe}(\text{NO})_3]^+$  complex, sterically encumbered by the wing-tips of the 1,3-bis(2,4,6-trimethylphenyl)imidazol-2-ylidene (IMes) ligand, could be readily isolated and manipulated in solution under ambient conditions.<sup>30</sup> The trinitrosyl iron moiety is diamagnetic and can be described as  $\{\text{Fe}(\text{NO})_3\}^{10}$ . This is consistent with the fact that the synthesis of the TNIC was carried out by isoelectronic replacement of CO in  $[(\text{NHC-Mes})\text{Fe}(\text{NO})_2(\text{CO})]$  by NO<sup>+</sup> (Figure 13). The substitutional lability of one NO ligand rendered the TNICs extremely valuable synthons as previously described.

#### ■ CONCLUDING REMARKS

Amplly displayed in the chemistry revealed by our studies is the capability of Fe(NO)<sub>2</sub> to exist in two redox levels while maintaining its integrity as a sterically rigid and intact, electron-delocalized unit. Its distinctive EPR (in its oxidized form) and

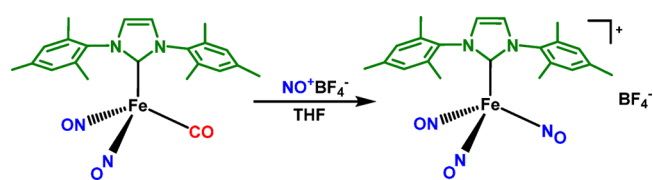


**Figure 13.** Synthesis of NHC-TNIC.<sup>30</sup>



IR (in both oxidized and reduced forms) spectroscopic signatures suggest more extensive investigations to better define roles for it in biochemistry and biology, as well as to develop its potential for identification of binding sites in proteins or other biomolecules.

With metallothiolates as ligands to  $\text{Fe}(\text{NO})_2$ , we uncovered a diiron complex with at least some ability for proton reduction electrocatalysis. The spectroscopic signatures, aided by computational support, helped define a mechanism that implicated redox activity in the DNIU as well as the redox active metallothiolate ligand. Remaining ill-defined are the positions of proton uptake, the factors that might favor expansion of the DNIU coordination sphere and the breaking of symmetry of the  $\text{Fe}(\text{NO})_2$  unit, and the role of hemilability of the  $\text{MN}_2\text{S}_2$  ligands. Pragmatically, the known  $\text{MN}_2\text{S}_2$  ligands offer a library of potential catalysts, for which the synthetic approaches we have outlined will be valuable. Thoughtful choices and educated guesses will optimize chances of success.

The ligand support afforded to the DNIU by NHCs demonstrated superior bonding compared with imidazoles, indicating stabilization by remote steric constraints likely realized for histidine in the restrictions of protein matrices. Such stabilization was critical for development of NHC-trinitrosyl iron complexes as valuable synthons and also as a controllable NO-release agent. The well-known ease of modifying the NHC ligands, for water solubilization, attachment to biomolecules, and immobilization on supports suitable for drug delivery, as well as possible expansion into other organometallic processes as evidenced by the observed tautomerization of imidazoles into NHCs, present vast opportunities for development.

## AUTHOR INFORMATION

### Corresponding Author

\*Marcetta Y. Darensbourg. E-mail: [marcetta@chem.tamu.edu](mailto:marcetta@chem.tamu.edu).

### Notes

The authors declare no competing financial interest.

### Biographies

**Randara Pulukkody** received her B.S. degree in chemistry from the University of Colombo, Sri Lanka, in 2009. She joined the M. Y. Darensbourg group at Texas A&M University as a Ph.D. student in 2010, where her dissertation work is focused on synthetic models of dinitrosyl iron complexes and reactivity studies thereof.

**Marcetta Y. Darensbourg**, Distinguished Professor of Chemistry at Texas A&M University, was trained as an organometallic chemist. With earlier research programs in low valent transition metal hydrides, the possibility of metal hydrides in nature, specifically as intermediates in hydrogenase metalloenzymes lured her into the field of bioorganometallic chemistry. There she found synthetic inspiration in the hydrogenase active sites and other diatomic ligand complexes of iron.

## ACKNOWLEDGMENTS

The original work from Texas A&M University described herein is largely attributable to the synthetic expertise and dedication of Dr. Hung-Chung Hsieh, currently at Tamkang University, Taiwan. Both M.Y.D. and Dr. Hsieh were inspired by the work of Prof. W.-F. Liaw. Funding from the National Science Foundation (Grant CHE-1266097) and the Robert A. Welch Foundation (Grant A-0924) is gratefully acknowledged.

## REFERENCES

- (1) Bagley, K. A.; Vangarderen, C. J.; Chen, M.; Duin, E. C.; Albracht, S. P. J.; Woodruff, W. H. Infrared Studies on the Interaction of Carbon-Monoxide with Divalent Nickel in Hydrogenase from Chromatium-Vinosum. *Biochemistry* **1994**, *33*, 9229–9236.
- (2) Nicolet, Y.; Lemon, B. J.; Fontecilla-Camps, J. C.; Peters, J. W. A Novel FeS Cluster in Fe-only Hydrogenases. *Trends Biochem. Sci.* **2000**, *25*, 138–143.
- (3) Volbeda, A.; Garcin, E.; Piras, C.; de Lacey, A. L.; Fernandez, V. M.; Hatchikian, E. C.; Frey, M.; Fontecilla-Camps, J. C. Structure of the [NiFe] Hydrogenase Active Site: Evidence for Biologically Uncommon Fe Ligands. *J. Am. Chem. Soc.* **1996**, *118*, 12989–12996.
- (4) Hsieh, C. H.; Ding, S. D.; Erdem, O. F.; Crouthers, D. J.; Liu, T. B.; McCrory, C. C. L.; Lubitz, W.; Popescu, C. V.; Reibenspies, J. H.; Hall, M. B.; Darensbourg, M. Y. Redox Active Iron Nitrosyl Units in Proton Reduction Electrocatalysis. *Nat. Commun.* **2014**, *5*, No. 3684.
- (5) Harmjanz, M.; Saak, W.; Haase, D.; Pohl, S. Aryl Isonitrile Binding to  $[\text{Fe}_4\text{S}_4]$  Clusters: Formation of  $[\text{Fe}_4\text{S}_4]^+$  and  $[\{\text{Fe}_4\text{S}_4\}_2]^{2+}$  Cores. *Chem. Commun.* **1997**, *10*, 951–952.
- (6) Lubitz, W.; Ogata, H.; Rudiger, O.; Reijerse, E. Hydrogenases. *Chem. Rev.* **2014**, *114*, 4081–4148.
- (7) Liaw, W. F.; Chiang, C. Y.; Lee, G. H.; Peng, S. M.; Lai, C. H.; Darensbourg, M. Y. Heterobimetallics of Nickel-Iron Dinitrosyl: Electronic Control by Chelate and Diatomic Ligands. *Inorg. Chem.* **2000**, *39*, 480–484.
- (8) Enemark, J. H.; Feltham, R. D. Principles of Structure, Bonding, and Reactivity for Metal Nitrosyl Complexes. *Coord. Chem. Rev.* **1974**, *13*, 339–406.
- (9) Ye, S. F.; Neese, F. The Unusual Electronic Structure of Dinitrosyl Iron Complexes. *J. Am. Chem. Soc.* **2010**, *132*, 3646–3647.
- (10) Vanin, A. F. In *Bioorganometallic Chemistry*; Wiley-VCH Verlag GmbH & Co. KGaA, Weinheim, Germany, 2015; pp 203–238.
- (11) Hickok, J. R.; Sahni, S.; Shen, H.; Arvind, A.; Antoniou, C.; Fung, L. W. M.; Thomas, D. D. Dinitrosyliron Complexes are the Most Abundant Nitric Oxide-Derived Cellular Adduct: Biological Parameters of Assembly and Disappearance. *Free Radical Biol. Med.* **2011**, *51*, 1558–1566.
- (12) Lewandowska, H.; Kalinowska, M.; Brzoska, K.; Wojciuk, K.; Wojciuk, G.; Kruszewski, M. Nitrosyl Iron Complexes-Synthesis, Structure and Biology. *Dalton Trans.* **2011**, *40*, 8273–8289.
- (13) Mulsch, A.; Mordvintsev, P.; Vanin, A. F.; Busse, R. The Potent Vasodilating and Guanylyl Cyclase Activating Dinitrosyl-Iron(II) Complex Is Stored in a Protein-Bound Form in Vascular Tissue and Is Released by Thiols. *FEBS Lett.* **1991**, *294*, 252–256.
- (14) Lok, H. C.; Sahni, S.; Richardson, V.; Kalinowski, D. S.; Kovacevic, Z.; Lane, D. J. R.; Richardson, D. R. Glutathione S-transferase and MRP1 Form an Integrated System Involved in the Storage and Transport of Dinitrosyl-Dithiolato Iron Complexes in Cells. *Free Radical Biol. Med.* **2014**, *75*, 14–29.
- (15) Cesareo, E.; Parker, L. J.; Pedersen, J. Z.; Nuccetelli, M.; Mazzetti, A. P.; Pastore, A.; Federici, G.; Accuri, A. M.; Ricci, G.; Adams, J. J.; Parker, M. W.; Lo Bello, M. Nitrosylation of Human Glutathione Transferase P1–1 with Dinitrosyl Diglutathionyl Iron Complex in Vitro and in Vivo. *J. Biol. Chem.* **2005**, *280*, 42172–42180.
- (16) Tsai, M.-L.; Tsou, C.-C.; Liaw, W.-F. Dinitrosyl Iron Complexes (DNICs): From Biomimetic Synthesis and Spectroscopic Characterization toward Unveiling the Biological and Catalytic Roles of DNICs. *Acc. Chem. Res.* **2015**, *48*, 1184–1193.
- (17) Tran, C. T.; Skodje, K. M.; Kim, E. In *Progress in Inorganic Chemistry*; Karlin, K. D., Ed.; John Wiley & Sons, Inc.: Hoboken, NJ, 2014; Vol. 59, pp 339–380.
- (18) Tonzetich, Z. J.; Do, L. H.; Lippard, S. J. Dinitrosyl Iron Complexes Relevant to Rieske Cluster Nitrosylation. *J. Am. Chem. Soc.* **2009**, *131*, 7964–7965.
- (19) Darnault, C.; Volbeda, A.; Kim, E. J.; Legrand, P.; Vernede, X.; Lindahl, P. A.; Fontecilla-Camps, J. C. Ni-Zn- $[\text{Fe}_4\text{S}_4]$  and Ni-Ni- $[\text{Fe}_4\text{S}_4]$  Clusters in Closed and Open  $\alpha$  Subunits Of Acetyl-CoA Synthase/Carbon Monoxide Dehydrogenase. *Nat. Struct. Mol. Biol.* **2003**, *10*, 271–279.

- (20) Huang, W. J.; Jia, J.; Cummings, J.; Nelson, M.; Schneider, G.; Lindqvist, Y. Crystal Structure of Nitrile Hydratase Reveals a Novel Iron Centre in a Novel Fold. *Structure* **1997**, *5*, 691–699.
- (21) Denny, J. A.; Darensbourg, M. Y. Metallothiolates as Ligands in Coordination, Bioinorganic and Organometallic Chemistry. *Chem. Rev.* **2015**, *115*, 5248–5273.
- (22) Miller, M. L.; Ibrahim, S. A.; Golden, M. L.; Darensbourg, M. Y. Adamantane-like Cluster Complexes of Mixed-Valent Copper–Copper and Nickel–Copper Thiolates. *Inorg. Chem.* **2003**, *42*, 2999–3007.
- (23) Hung, M.-C.; Tsai, M.-C.; Lee, G.-H.; Liaw, W.-F. Transformation and Structural Discrimination between the Neutral  $\{\text{Fe}(\text{NO})_2\}^{10}$  Dinitrosyliron Complexes (DNICs) and the Anionic/Cationic  $\{\text{Fe}(\text{NO})_2\}^9$  DNICs. *Inorg. Chem.* **2006**, *45*, 6041–6047.
- (24) Hess, J. L.; Hsieh, C. H.; Reibenspies, J. H.; Darensbourg, M. Y. N-Heterocyclic Carbene Ligands as Mimics of Imidazoles/Histidine for the Stabilization of Di- and Trinitrosyl Iron Complexes. *Inorg. Chem.* **2011**, *50*, 8541–8552.
- (25) McBride, D. W.; Stafford, S. L.; Stone, F. G. A. Chemistry of the Metal Carbonyls. XVI. Synthesis of Dicarbonyldinitrosyliron(0). *Inorg. Chem.* **1962**, *1*, 386–388.
- (26) Hsieh, C.-H.; Chupik, R. B.; Brothers, S. M.; Hall, M. B.; Darensbourg, M. Y. cis-Dithiolatonicel as Metalloligand to Dinitrosyl Iron Units: The Di-metallic Structure of  $\text{Ni}(\mu\text{-SR})[\text{Fe}(\text{NO})_2]$  and an Unexpected, Abbreviated Metaladamantyl Cluster,  $\text{Ni}_2(\mu\text{-SR})_4[\text{Fe}(\text{NO})_2]_3$ . *Dalton Trans.* **2011**, *40*, 6047–6053.
- (27) Pinder, T. A.; Montalvo, S. K.; Hsieh, C. H.; Lunsford, A. M.; Bethel, R. D.; Pierce, B. S.; Darensbourg, M. Y. Metallothiolates as Ligands to Dinitrosyl Iron Complexes: Toward the Understanding of Structures, Equilibria, and Spin Coupling. *Inorg. Chem.* **2014**, *53*, 9095–9105.
- (28) Anderson, J. S.; Hieber, W. Mitarbeitern Über ein flüchtiges Eisen–Nitrosocarbonyl,  $\text{Fe}(\text{CO})_2(\text{NO})_2$ . 17. Abhandlung über Metallcarbonyle. *Z. Anorg. Allg. Chem.* **1932**, *208*, 238–248.
- (29) Rauchfuss, T. B.; Weatherill, T. D. Roussin's Red Salt Revisited: Reactivity of  $\text{Fe}_2(\mu\text{-E})_2(\text{NO})_4^2-$  (E = S, Se, Te) and Related Compounds. *Inorg. Chem.* **1982**, *21*, 827–830.
- (30) Hsieh, C. H.; Darensbourg, M. Y. A  $\{\text{Fe}(\text{NO})_3\}^{10}$  Trinitrosyliron Complex Stabilized by an N-Heterocyclic Carbene and the Cationic and Neutral  $\{\text{Fe}(\text{NO})_2\}^{9/10}$  Products of Its NO Release. *J. Am. Chem. Soc.* **2010**, *132*, 14118–14125.
- (31) Hsieh, C. H.; Chupik, R. B.; Pinder, T. A.; Darensbourg, M. Y. Dinitrosyl Iron Adducts of  $(\text{N}_2\text{S}_2)\text{M}(\text{NO})$  Complexes (M = Fe, Co) as Metallothiolate Ligands. *Polyhedron* **2013**, *58*, 151–155.
- (32) Chiang, C. Y.; Miller, M. L.; Reibenspies, J. H.; Darensbourg, M. Y. Bismercaptoethanediazacyclooctane as a  $\text{N}_2\text{S}_2$  Chelating Agent and Cys-x-Cys Mimic for  $\text{Fe}(\text{NO})$  and  $\text{Fe}(\text{NO})_2$ . *J. Am. Chem. Soc.* **2004**, *126*, 10867–10874.
- (33) Chiang, C. Y.; Darensbourg, M. Y. Iron Nitrosyl Complexes as Models for Biological Nitric Oxide Transfer Reagents. *J. Biol. Inorg. Chem.* **2006**, *11*, 359–370.
- (34) Wang, R.; Camacho-Fernandez, M. A.; Xu, W.; Zhang, J.; Li, L. Neutral and Reduced Roussin's Red Salt Ester  $[\text{Fe}_2(\mu\text{-RS})_2(\text{NO})_4]$  (R = n-Pr, t-Bu, 6-methyl-2-pyridyl and 4,6-dimethyl-2-pyrimidyl): Synthesis, X-Ray Crystal Structures, Spectroscopic, Electrochemical and Density Functional Theoretical Investigations. *Dalton Trans.* **2009**, *5*, 777–786.
- (35) Reginato, N.; McCrory, C. T. C.; Pervitsky, D.; Li, L. J. Synthesis, X-ray Crystal Structure, and Solution Behavior of  $\text{Fe}(\text{NO})_2(1\text{-Meim})_2$ : Implications for Nitrosyl Non-heme-iron Complexes with  $g=2.03$ . *J. Am. Chem. Soc.* **1999**, *121*, 10217–10218.
- (36) Li, L. J. Some Coordination Chemistry of Non-heme Iron Nitrosyl Complexes. *Comments Inorg. Chem.* **2002**, *23*, 335–353.
- (37) Hopkinson, M. N.; Richter, C.; Schedler, M.; Glorius, F. An Overview of N-heterocyclic Carbenes. *Nature* **2014**, *510*, 485–496.
- (38) Riener, K.; Haslinger, S.; Raba, A.; Hogerl, M. P.; Cokoja, M.; Herrmann, W. A.; Kuhn, F. E. Chemistry of Iron N-Heterocyclic Carbene Complexes: Syntheses, Structures, Reactivities, and Catalytic Applications. *Chem. Rev.* **2014**, *114*, 5215–5272.
- (39) Jenkins, R. M.; Singleton, M. L.; Leamer, L. A.; Reibenspies, J. H.; Darensbourg, M. Y. Orientation and Stereodynamic Paths of Planar Monodentate Ligands in Square Planar Nickel  $\text{N}_2\text{S}$  Complexes. *Inorg. Chem.* **2010**, *49*, 5503–5514.
- (40) Hess, J. L.; Hsieh, C. H.; Brothers, S. M.; Hall, M. B.; Darensbourg, M. Y. Self-Assembly of Dinitrosyl Iron Units into Imidazolate-Edge-Bridged Molecular Squares: Characterization Including Mossbauer Spectroscopy. *J. Am. Chem. Soc.* **2011**, *133*, 20426–20434.
- (41) Chaudhuri, P.; Karpenstein, I.; Winter, M.; Lengen, M.; Butzlaff, C.; Bill, E.; Trautwein, A. X.; Floerke, U.; Haupt, H. J. An Imidazolate-bridged Tetranuclear Copper(II) Complex: Synthesis, Magnetic and EPR Studies, and Crystal Structure of  $[\text{L}_4\text{Cu}_4(\text{Im})_4](\text{ClO}_4)_4 \cdot 2\text{H}_2\text{O}$  (L = 1,4,7-triazacyclononane, Im = imidazolate anion). *Inorg. Chem.* **1993**, *32*, 888–894.
- (42) Pulukkody, R.; Kyran, S. J.; Bethel, R. D.; Hsieh, C. H.; Hall, M. B.; Darensbourg, D. J.; Darensbourg, M. Y. Carbon Monoxide Induced Reductive Elimination of Disulfide in an N-Heterocyclic Carbene (NHC)/Thiolate Dinitrosyl Iron Complex (DNIC). *J. Am. Chem. Soc.* **2013**, *135*, 8423–8430.
- (43) Pulukkody, R.; Kyran, S. J.; Drummond, M. J.; Hsieh, C. H.; Darensbourg, D. J.; Darensbourg, M. Y. Hammett Correlations as Test of Mechanism of CO-Induced Disulfide Elimination from Dinitrosyl Iron Complexes. *Chem. Sci.* **2014**, *5*, 3795–3802.
- (44) Hsieh, C. H.; Pulukkody, R.; Darensbourg, M. Y. A Dinitrosyl Iron Complex as a Platform for Metal-Bound Imidazole to N-Heterocyclic Carbene Conversion. *Chem. Commun.* **2013**, *49*, 9326–9328.
- (45) Chong, K. S.; Rettig, S. J.; Storr, A.; Trotter, J. Synthesis and Structure of 3,5-Dimethylpyrazolyl Iron and Cobalt Dinitrosyl Dimers. *Can. J. Chem.* **1979**, *57*, 3119–3125.
- (46) Holloway, L. R.; Clough, A. J.; Li, J. Y.; Tao, E. L.; Tao, F. M.; Li, L. J. A Combined Experimental and Theoretical Study of Dinitrosyl Iron Complexes Containing Chelating Bis(diphenyl)phosphinoX (X = Benzene, Propane and Ethylene): X-Ray Crystal Structures and Properties Influenced by the Presence or Absence of Pi-Bonds in Chelating Ligands. *Polyhedron* **2014**, *70*, 29–38.
- (47) Sini, G.; Eisenstein, O.; Crabtree, R. H. Preferential C-binding versus N-binding in Imidazole Depends on the Metal Fragment Involved. *Inorg. Chem.* **2002**, *41*, 602–604.
- (48) Kajimura, M.; Fukuda, R.; Bateman, R. M.; Yamamoto, T.; Suematsu, M. Interactions of Multiple Gas-Transducing Systems: Hallmarks and Uncertainties of CO, NO, and  $\text{H}_2\text{S}$  Gas Biology. *Antioxid. Redox Signaling* **2010**, *13*, 157–192.
- (49) Hayton, T. W.; McNeil, W. S.; Patrick, B. O.; Legzdins, P. Toward Binary Nitrosyls: Distinctly Bent Fe–N–O Linkages in Base-Stabilized  $\text{Fe}(\text{NO})_3^+$  Complexes. *J. Am. Chem. Soc.* **2003**, *125*, 12935–12944.
- (50) Dillinger, S. A. T.; Schmalle, H. W.; Fox, T.; Berke, H. Developing Iron Nitrosyl Complexes as NO Donor Prodrugs. *Dalton Trans.* **2007**, *32*, 3562–3571.